Analysis of a point-source integrating-cavity absorption meter

Robert A. Leathers, T. Valerie Downes, and Curtiss O. Davis

We evaluate the theoretical performance of a point-source integrating-cavity absorption meter (PSICAM) with Monte Carlo simulations and a sensitivity analysis. We quantify the scattering errors, verifying that they are negligible for most ocean optics applications. Although the PSICAM detector response is highly sensitive to the value of the wall reflectivity, the absorption of an unknown fluid can be accurately determined with a PSICAM if appropriate reference solution(s) are chosen. We also quantify the error that results if the source is not perfectly isotropic, finding that moderate amounts of source anisotropy can be tolerated provided that the detector is properly located with respect to the source.

OCIS codes: 010.4450, 030.5260, 030.5620, 120.4640, 300.1030.

1. Introduction

The measurement of light absorption by seawater and its components is of great interest for oceanography and for optical remote sensing of the ocean. Biological oceanographers measure the absorption of light by phytoplankton to quantify photosynthesis; chemical oceanographers are concerned with the absorption of light by organic compounds and the photooxidation of those compounds; and physical oceanographers measure the absorption of energy by surface waters and its role in the heating of the surface layer and the formation of the thermocline. Optical oceanographers are concerned about all these processes as well as use of spectral absorption measurements to identify and quantify optically active components in the water.

There are several methods for determining the absorption coefficient of ocean waters. The most widely used approach is the quantitative filter technique,[1] in which water samples are concentrated onto glass-fiber filters and the absorption of the resulting filters and filtrate are measured separately in a spectrophotometer. This method requires corrections for scattering errors associated with the filter and for scattering errors in the spectrophotometric measurement of the filtrate. Because of its convenience compared with the quantitative filter technique, use of *in situ* absorption meters, in particular the ac-9 (WET Labs, Inc., Philomath, Oregon),[2,3] is becoming increasingly popular. These instruments measure the attenuation of an active light source through a volume of seawater, but, like a spectrophotometer, must be corrected for scattering errors. A third approach to determining the absorption coefficient of seawater is to measure the natural light within the water column and to invert the radiative transfer equation to calculate the values of the water's optical properties that are consistent with the observed light measurements.[4,5] The primary difficulty with this approach is the need to remove numerically or analytically the effects of the boundary conditions on the light field.

An alternative to these three approaches is use of an integrating-cavity absorption meter (ICAM), which is the focus of this research. The motivation of this approach is to obtain a measurement that is insensitive to scattering. The water sample is actively illuminated in the cavity of the ICAM, the walls of which are made of a highly reflective material so that the resulting light field within the cavity is nearly uniform. The absorption of the sample is taken to be the power input to the ICAM minus either the measured or the calculated losses at the cavity wall.

Elterman[6] suggested the use of a highly reflective Lambertian cavity to obtain a scattering-insensitive measurement of the absorption coefficient of a solid material. A small sample of the material was placed in an otherwise empty cavity, and the light source and detector were placed at the cavity walls. Fry and Kattawar[7,8] later adapted this approach for determining the absorption coefficient of seawater.

The authors are with the U.S. Naval Research Laboratory, Code 7212, 4555 Overlook Avenue, S.W., Washington, D.C. 20375. The e-mail address for R. Leathers is leathers@rsd.nrl.navy.mil.

Received 24 April 2000; revised manuscript received 28 August 2000.

Their configuration consists of a cavity completely filled with the water sample and a second integrating cavity surrounding the first. An isotropic light field is generated between the two cavities that diffuses into the inner cavity, providing to the inner cavity a diffuse light source that is uniform over the cavity walls. Kirk[9] proposed that the two cavities be made spherical and concentric, making it possible to model the relationship analytically between the absorption coefficient and the ICAM detector response.

Kirk[10] later proposed a different arrangement in which the spherical cavity containing the water sample is illuminated with an isotropic source at the center of the sphere. The primary advantage of this point-source integrating-cavity absorption meter (PSICAM) over the concentric cavity design is the elimination of the outer cavity, which is difficult to construct. Kirk[10] provides equations for obtaining the absorption coefficient with a PSICAM and includes some analysis of the design.

Here we extend Kirk's PSICAM analysis in preparation for the construction of a prototype instrument that will be used at the U.S. Naval Research Laboratory for the investigation of coastal ocean waters. Kirk's[9,10] equations for the operation of a PSICAM, which ignore scattering effects, are reviewed in Section 2. The errors in these equations that are due to scattering are quantified in Section 3, and a sensitivity analysis of the equations is provided in Section 4. In Section 5 we investigate the error that is introduced when the light source is not perfectly isotropic. A summary of our conclusions is provided in Section 6.

2. Basic Equations

The outwardly directed irradiance F_0 at the inner wall of a perfectly symmetrical PSICAM is proportional to the average number of times a photon collides with the wall, N_C, before being absorbed either by the fluid in the cavity or by the cavity wall.[9,10] The transmittance T_{AB} that is the ratio of the measured values of F_0 when the cavity is filled with samples A and B, respectively, is therefore

$$T_{AB} = \frac{F_0^A}{F_0^B} = \frac{N_C^A}{N_C^B}. \tag{1}$$

Note that the effects of the source strength and detector gain on F_0 cancel out when forming the ratio T_{AB}. The value of N_C depends on three quantities: (1) the probability P_0 that a photon leaving the source at the center reaches the wall (i.e., without being absorbed by the fluid), (2) the wall reflectivity ρ, and (3) the probability P_s that a photon leaving the wall will return to the wall. The value of N_C equals the number of photons reaching the wall directly from the source plus the number of photons colliding with the wall for a second time plus the number colliding with the wall for a third time, etc.:

$$N_C = P_0 + P_0\rho P_s + P_0\rho^2 P_s^2 + \ldots = P_0 \sum_{n=0}^{\infty} (\rho P_s)^n = P_0/(1 - \rho P_s). \tag{2}$$

Therefore

$$T_{AB} = \frac{P_0^A(1 - \rho P_s^B)}{P_0^B(1 - \rho P_s^A)}. \tag{3}$$

For a central point source the value of P_0 for a nonscattering solution is[10]

$$P_0(a, r) = \exp(-ar), \tag{4}$$

where a is the absorption coefficient of the sample and r is the inner radius of the PSICAM cavity. However, if the source is generated with a diffusing sphere that has a radius r_s that is significantly large compared to the cavity radius, then we should take P_0 to be

$$P_0(a, r_0) = \exp(-ar_0), \tag{5}$$

where $r_0 = r - r_s$. For diffuse light leaving the spherical cavity wall the value of P_s for a nonscattering fluid is[9]

$$P_s(a, r) = \frac{1}{2a^2r^2}[1 - \exp(-2ar)(2ar + 1)]. \tag{6}$$

The size of the source is unlikely to be significant for P_s provided that the source material is nonabsorbing. For very small values of (ar), for which $P_s \approx 1$, Eq. (6) is difficult to evaluate; however, the power series[9]

$$P_s(a, r) = 1 - \frac{4}{3}(ar) + (ar)^2 - \frac{8}{15}(ar)^3 + \cdots 2(-2ar)^n\left[\frac{1}{(n+1)!} - \frac{1}{(n+2)!}\right] + \cdots \tag{7}$$

converges rapidly for very small values of (ar). From Eqs. (3), (5), and (6), the transmittance of a nonscattering fluid in a PSICAM with a diffuse cavity wall is

$$T_{AB} = \exp[-r_0(a_A - a_B)]\left[\frac{1 - \rho P_s(a_B, r)}{1 - \rho P_s(a_A, r)}\right], \tag{8}$$

with $P_s(a, r)$ given by Eq. (6).

Kirk[10] indicates that both P_0 and P_s are insensitive to the presence of scattering for most practical ocean optics purposes and that Eqs. (6) and (8) can therefore be applied to seawater samples even though scattering was ignored in their derivation. In Section 3 we quantify the magnitude of the scattering error in these equations for a large range of physical parameters.

Equation (8) can be used in two ways. First, when the absorption coefficients of samples A and B are known the wall reflectivity can be determined from the measurement of T_{AB} with the solution[10] of Eq. (8):

$$\rho = \frac{T_{AB}\exp(-a_B r_0) - \exp(-a_A r_0)}{T_{AB}\exp(-a_B r_0)P_s(a_A, r) - \exp(-a_A r_0)P_s(a_B, r)}. \tag{9}$$

Second, from Eq. (8) we can express the transmittance T of a fluid of interest with unknown absorption coefficient a with respect to a reference sample R with known absorption coefficient a_{ref}:

$$T = \exp[-r_0(a - a_{\mathrm{ref}})]\left[\frac{1 - \rho P_s(a_{\mathrm{ref}}, r)}{1 - \rho P_s(a, r)}\right]. \quad (10)$$

The value of a can therefore be determined from the measurement of T with an iterative solution of Eq. (10).

In summary, we can determine the unknown absorption coefficient a of a sample of interest by (1) measuring the irradiance values at the PSICAM cavity wall with the cavity filled with solutions A and B (of known absorption coefficients a_A and a_B); (2) forming the ratio T_{AB} from these two measurements [Eq. (1)]; (3) computing ρ with Eq. (9); (4) measuring the irradiance at the PSICAM cavity wall both with the cavity filled with the sample of interest (with unknown absorption coefficient a) and with the cavity filled with reference solution R (with known absorption coefficient a_{ref}); (5) forming the ratio T of these two measurements; and (6) solving Eq. (10) for a. Note that the required number of reference solutions with the known absorption coefficient can be reduced from three (R, A, and B) to two (R and A) if solutions B and R are taken to be the same. Furthermore, if the value of ρ is known from direct measurement, only steps (4)–(6) are needed and we require only one reference solution (R).

3. Scattering Effects

Equations (5) and (6) for the probabilities of photon survival P_0 and P_s were derived for nonscattering absorbers. In Monte Carlo simulations, Kirk[9,10] found P_0 and P_s for seawater to be insensitive to the value of b. However, in general, the presence of scattering decreases the value of P_0 by increasing the effective path length of each photon from the source to the wall. Scattering also alters the effective path length of a photon as it travels from the wall back to the wall. Therefore there must be limits on the values of a, b, and r for which the application of Eqs. (5) and (6) is valid.

We examined the effect of scattering on the values of P_0, P_s, and N_C with Monte Carlo simulations. These simulations were performed for both isotropic scattering and for scattering given by the average of Petzold's seawater measurements in San Diego Harbor.[11] The Petzold scattering phase function is highly peaked in the forward direction, with backscattering representing only approximately 2% of the total scattering (as opposed to 50% for isotropic scattering). The values of P_0 and P_s were computed separately, and Eq. (2) was used to determine N_C for specific values of ρ. The key equations for the Monte Carlo simulations are given in Appendix A.

Because the value of P_0 decreases with increasing values of b, Eq. (5) overestimates the true value of P_0. The percentage error in Eq. (5) was found to increase approximately linearly with respect to b and to be greatest for large values of a and r_0. The error for Petzold scattering was much smaller than that for isotropic scattering because for Petzold scattering the photons are scattered predominantly in the near-forward direction. For example, the percentage error in P_0 determined from Eq. (5) is shown versus b (log scale) in Fig. 1 for radius $r_0 = r = 0.05$ m, wall reflectivity $\rho = 0.99$, and absorption coefficient $a = 1$ m^{-1}. For isotropic scattering, the error in Eq. (5) is approximately 0.9% and 11% for $b = 10$ m^{-1} and $b = 100$ m^{-1}, respectively, whereas for Petzold scattering the error in Eq. (5) is only approximately 0.04% and 0.6%, respectively. For $a = 0.1$ m^{-1}, the errors were only approximately one tenth of those for $a = 1$ m^{-1}.

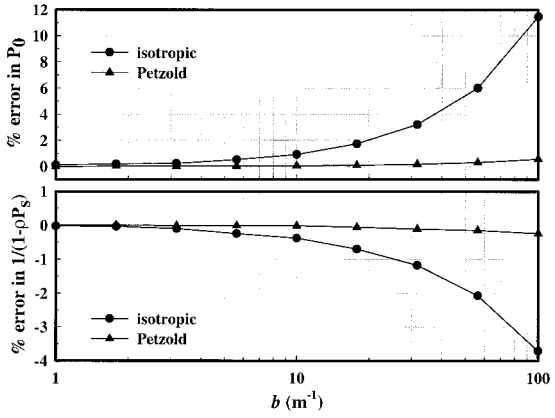

Fig. 1. Percentage scattering errors in P_0 and $1/(1 - \rho P_s)$ for isotropic and Petzold scattering when the probabilities of source-to-wall photon survival (P_0) and wall-to-wall photon survival (P_s) are computed with Eqs. (5) and (6) with $a = 1.0$ m^{-1} and $r = r_0 = 0.05$ m.

When a photon traveling from the wall back to the wall is scattered, its effective path length may be smaller or larger than it would have been if unscattered, depending on where, and into which direction, it is scattered. For small values of a, b, and r it was found that the overall (statistical) scattering effect is negligible. For large values of a, b, or r, however, it is more likely that a photon will be scattered back to the wall near where it left, thus increasing the value of P_s, than it is that its path length will be increased by scattering. Equation (6) therefore underestimates the true value of P_s for large values of a, b, or r. Even if the scattering error in P_s appears to be insignificantly small, it may nonetheless have a significant effect on the total PSICAM response through the term $1/(1 - \rho P_s)$. The percentage error in $1/(1 - \rho P_s)$ is shown in Fig. 1 for $r = 0.05$ m, $\rho = 0.99$, and $a = 1$ m^{-1}. Its magnitude increases approximately linearly with increasing values of b but is approximately one third that of the error in P_0.

Because scattering affects P_0 and P_s in opposite ways, the percentage error in F_0 (which equals the percentage error in N_C) is smaller than that in either P_0 or P_s. The error in the PSICAM response predicted by Eqs. (2), (4), and (6) is shown in Fig. 2 for isotropic scattering and in Fig. 3 for Petzold scattering. The scattering effect on F_0 was found to be

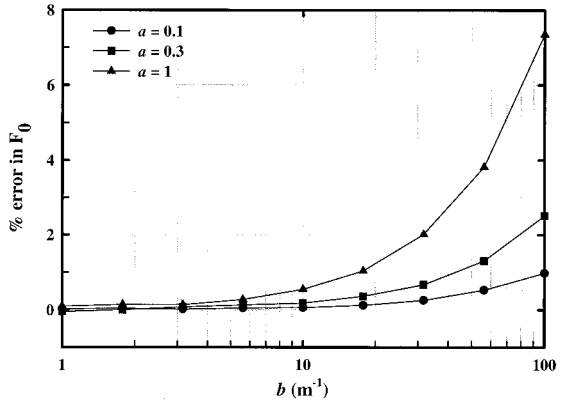

Fig. 2. Percentage error in the PSICAM response predicted by Eqs. (2), (4), and (6) that is due to the presence of isotropic scattering for $r = 0.05$ m and $\rho = 0.99$.

insignificant for most oceanic problems; even for the extremely large value of $b = 100$, the error in F_0 for Petzold scattering is less than 0.35% when $a < 1\ \mathrm{m}^{-1}$. However, the scattering effects may be important for the infrared wavelengths (for which $a > 1\ \mathrm{m}^{-1}$) or for other PSICAM applications that have a less anisotropic scattering phase function than water or have significantly larger values of a, r, or b than those used in Fig. 3.

4. Sensitivity Analysis

The determination of the absorption coefficient of a fluid sample with Eq. (10) requires several measurements, the uncertainties of which result in a total uncertainty in the estimate of a. Here we examine the sensitivities of the determined value of a to these measurements. We first conduct this analysis for the mode of PSICAM operation in which the cavity-wall reflectivity ρ is assumed to be known from direct measurement. We then focus on the mode of operation in which ρ is instead determined from PSICAM measurements of two nonscattering samples of known absorption coefficient values [i.e., with Eq. (9)].

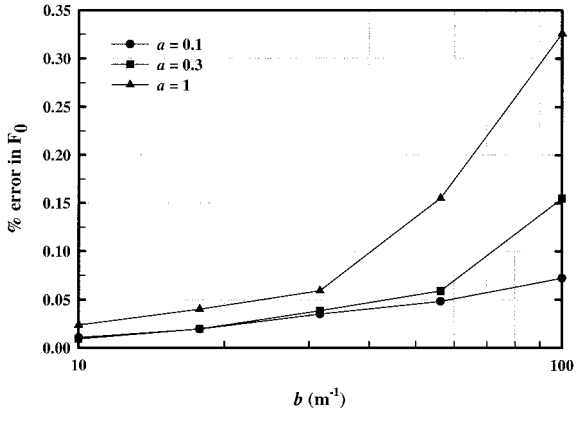

Fig. 3. Percentage error in the PSICAM response predicted by Eqs. (2), (4), and (6) that is due to the presence of seawater scattering for $r = 0.05$ m and $\rho = 0.99$.

The analytical forms of the sensitivity coefficients derived in this section are valid for any PSICAM application; however, the ranges of the physical parameters in our examples, figures, and discussions are chosen to be consistent with applications to coastal ocean waters, visible wavelengths, and a PSICAM cavity made with Spectralon (Labsphere, Inc., North Sutton, N.H.). The value of the absorption coefficient of pure seawater for light in the 400–700-nm range has a minimum value of $0.014\ \mathrm{m}^{-1}$ (at 430 nm) and a maximum value of $0.65\ \mathrm{m}^{-1}$ (at 700 nm). The value of a in this wavelength range for natural ocean waters is typically between 0.1 and 1.0 m^{-1}, depending on the wavelength and the concentrations of phytoplankton, suspended sediments, and suspended and dissolved organic material. The reflectivity of Spectralon is approximately $\rho = 0.99$.

A. Known ρ

If the values of ρ, r, and a_{ref} are known, we can determine the absorption coefficient of a fluid sample by measuring T [Eq. (1)] and then numerically solving Eq. (10). Here we examine the sensitivity of the value of a obtained from Eq. (10) to the four quantities T, ρ, r, and a_{ref}. In general the values of the four sensitivity coefficients $\partial a/\partial T$, $\partial a/\partial \rho$, $\partial a/\partial r$, and $\partial a/\partial a_{\mathrm{ref}}$ depend on the four physical parameters ρ, r, a_{ref}, and a.

For T given by Eq. (10) and P_s given by Eq. (6),

$$\frac{T}{a}\frac{\partial a}{\partial T} = -\frac{2a^2r^2 - \rho[1 - (2ar + 1)\exp(-2ar)]}{2a^3r^3 - \rho[(2a^2r^2 + 3ar + 2)\exp(-2ar) - 2 + ar]}, \tag{11}$$

where we have ignored the size of the source. Note that on the right-hand side of Eq. (11) the parameters a and r exist only as the product (ar). We show the normalized form of the sensitivity coefficient in Eq. (11) because it is conveniently independent of a_{ref}. We can find the value of $\partial a/\partial T$ by multiplying Eq. (11) by (a/T) with T replaced by the expression in Eq. (10), which introduces a dependence on a_{ref}. The sensitivity coefficient of a with respect to ρ can be found from Eq. (10) with

$$\frac{\partial a}{\partial \rho} = -\frac{\partial T/\partial \rho}{\partial T/\partial a}. \tag{12}$$

Likewise

$$\frac{\partial a}{\partial r} = -\frac{\partial T/\partial r}{\partial T/\partial a}, \quad \frac{\partial a}{\partial a_{\mathrm{ref}}} = -\frac{\partial T/\partial a_{\mathrm{ref}}}{\partial T/\partial a}. \tag{13}$$

Table 1 gives the values of the four sensitivity coefficients in both their unnormalized and their normalized form for the example cases of $a = 0.2\ \mathrm{m}^{-1}$, $a_{\mathrm{ref}} = 0.02\ \mathrm{m}^{-1}$, $r = 0.05$ m, and $\rho = 0.99$. We verified these coefficients with MAPLE V (Waterloo Maple, Inc., Waterloo, Ontario) by solving Eq. (10) with

Table 1. Sensitivity Coefficients for the Determination of a with Eqs. (6) and (10) when ρ is Known[a]

Coefficient	Value
$\partial a/\partial T$	$-0.72\ \mathrm{m}^{-1}$
$\partial a/\partial \rho$	$-16\ \mathrm{m}^{-1}$
$\partial a/\partial r$	$-3.2\ \mathrm{m}^{-2}$
$\partial a/\partial a_{\mathrm{ref}}$	2.1
$(T/a)(\partial a/\partial T)$	−1.7
$(\rho/a)(\partial a/\partial \rho)$	−79
$(r/a)(\partial a/\partial r)$	−0.79
$(a_{\mathrm{ref}}/a)(\partial a/\partial a_{\mathrm{ref}})$	0.21

[a] $a = 0.2\ \mathrm{m}^{-1}$, $a_{\mathrm{ref}} = 0.02\ \mathrm{m}^{-1}$, $r = 0.05$ m, and $\rho = 0.99$.

and without a small error in each parameter. Each unnormalized sensitivity coefficient gives the ratio of the absolute error in a to the absolute error in the parameter causing the error in a, whereas each normalized sensitivity coefficient gives the ratio of the percentage error in a to the percentage error in the given parameter. It can be seen from Table 1 that the value of a is most sensitive to ρ; for the parameter values used in Table 1, a 1% error in ρ would cause nearly an 80% error in a. The values of the sensitivity coefficients of a with respect to T, a_{ref}, and r are much smaller but nonetheless potentially significant. Letting ΔT represent the uncertainty in the measurement of T and $\Delta\rho$ represent the uncertainty in the measurement of ρ, etc., the total uncertainty in our computed value of a is[12]

$$\Delta a = \left[\left(\frac{\partial a}{\partial T}\right)^2 (\Delta T)^2 + \left(\frac{\partial a}{\partial \rho}\right)^2 (\Delta\rho)^2 + \left(\frac{\partial a}{\partial r}\right)^2 (\Delta r)^2 + \left(\frac{\partial a}{\partial a_{\mathrm{ref}}}\right)^2 (\Delta a_{\mathrm{ref}})^2\right]^{1/2}. \quad (14)$$

If, for the example used in Table 1, we measure r (0.050 m) to ±0.1 mm, ρ (0.990) to ±0.002, a_{ref} (0.020 m^{-1}) to ±0.005 m^{-1}, and the corresponding value of T (0.486) to 1% (i.e., F_0 is measured to ±0.5%), then from Eq. (14) and Table 1

$$\begin{aligned}\Delta a &= \{[(0.71)(0.00486)]^2 + [(16)(0.002)]^2 + [(3.2)\\ &\quad \times (0.0001)]^2 + [(2.1)(0.005)]^2\}^{1/2}\ \mathrm{m}^{-1}\\ &= (1.2\times 10^{-5} + 1.0\times 10^{-3} + 1.0\times 10^{-7}\\ &\quad + 1.1\times 10^{-4})^{1/2}\ \mathrm{m}^{-1}\\ &= 0.034\ \mathrm{m}^{-1}. \quad (15)\end{aligned}$$

Therefore our computed value of a would be $0.200 \pm 0.049\ \mathrm{m}^{-1}$, with the uncertainty due primarily to the measurements of ρ and a_{ref} and the uncertainty in r being insignificant.

We are perhaps more interested in the absolute uncertainty in a that is due to the relative (percentage) uncertainty in T, which is quantified by the term $(T)(\partial a/\partial T)$, than in either $(\partial a/\partial T)$ or $(T/a)(\partial a/\partial T)$. We can find $(T)(\partial a/\partial T)$ by simply multiplying Eq. (11) by a, and the term is shown versus a in Fig. 4. It is negative, indicating that the value of a will be underestimated if the measured value of T is greater than the true value and vice versa. It can be seen from Fig. 4 that $|T(\partial a/\partial T)|$ increases approximately linearly with increasing values of a and decreases with increasing values of r and ρ. It was found that $|T(\partial a/\partial T)|$ is relatively insensitive to the value of r for r greater than approximately 0.02 but increases rapidly with decreasing r for $r < 0.02$. The increase in $|T(\partial a/\partial T)|$ with decreasing ρ is approximately linear.

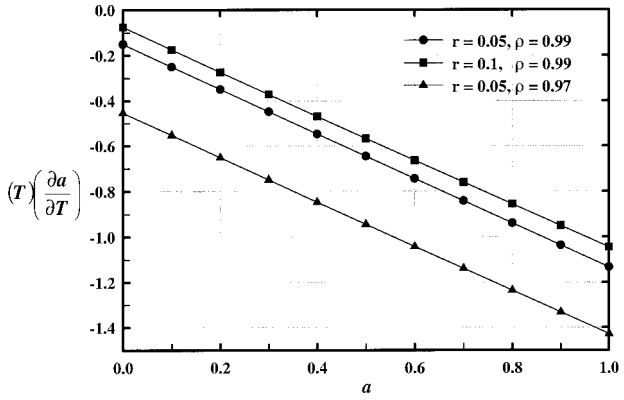

Fig. 4. Seminormalized sensitivity coefficient $(T)(\partial a/\partial T)$ (m^{-1}) versus a (m^{-1}).

The value of $\partial a/\partial \rho$ (Fig. 5) equals zero when $a = a_{\mathrm{ref}}$ and decreases approximately linearly with increasing a. Increasing a_{ref} or decreasing ρ moves the slope of the $(\partial a/\partial \rho)$ curve versus the a curve toward zero. Increasing r also moves the slope toward zero; however, the effect is small and is not illustrated in Fig. 5. Similarly the value of $\partial a/\partial r$ (Fig. 6) equals zero when $a = a_{\mathrm{ref}}$ and decreases approximately linearly with increasing a. The slope of $(\partial a/\partial r)$ versus a is steepest for small values of a_{ref}. The value of $\partial a/\partial a_{\mathrm{ref}}$ (Fig. 7) equals unity when $a = a_{\mathrm{ref}}$, increases approximately linearly with a, and is largest for small values of a_{ref}. It was found that the slope of the $(\partial a/\partial a_{\mathrm{ref}})$ curve versus the a curve increases when the value of ρ or r increases.

It is important to note from Figs. 5–7 that the value of a_{ref} has a dramatic effect on the overall uncertainty

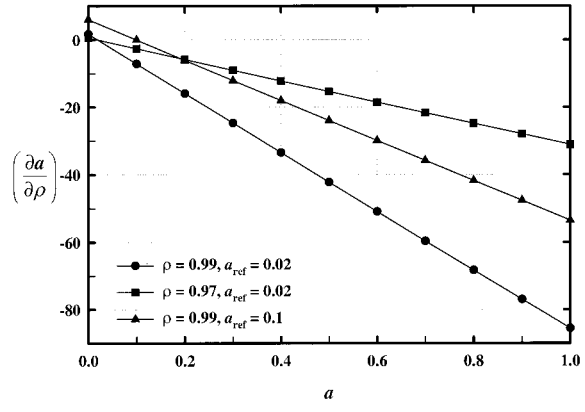

Fig. 5. Sensitivity coefficient $\partial a/\partial \rho$ (m^{-1}) versus a (m^{-1}) for $r = 0.05$ m.

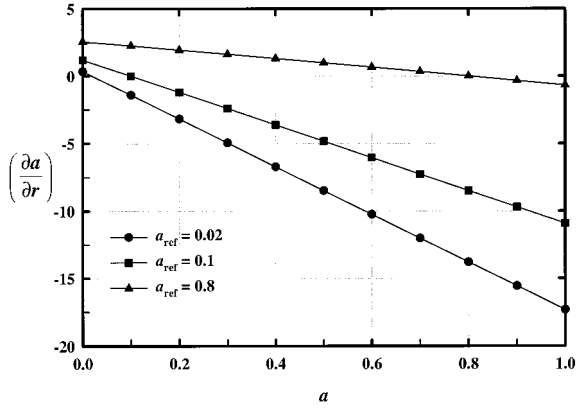

Fig. 6. Sensitivity coefficient $\partial a/\partial r$ (m^{-2}) versus a (m^{-1}) when ρ is known for $r = 0.05$ m and ρ = 0.99.

in a. In particular, we can reduce both sensitivity coefficients $\partial a/\partial \rho$ (Fig. 5) and $\partial a/\partial r$ (Fig. 6) to values near zero by taking $a_{\text{ref}} \approx a$. Although the values of r and ρ are generally fixed once a PSICAM is constructed, we can control the value of a_{ref} by varying the concentration of a nonscattering dye. We could obtain the most precise determination of a by first measuring F_0 for the unknown sample and then by adjusting the dye concentration in the reference solution as many times as necessary until $T = 1$ (i.e., $a_{\text{ref}} = a$). In this way a reference solution would be produced that has the same absorption coefficient as the sample of interest but presumably has a much smaller scattering coefficient. We could then measure the value of $a = a_{\text{ref}}$ by placing the reference solution in a spectrophotometer. The total uncertainty in a would be approximately equal to that in a_{ref} ($\partial a/\partial a_{\text{ref}} = 1$ when $a_{\text{ref}} = a$) plus that due to the uncertainty in the measurement of T[$T(\partial a/\partial T)$ is independent of the value of a_{ref}]. If a_{ref} in the example in Eq. (15) were changed to $a_{\text{ref}} = a$, the uncertainty in a would be reduced from 0.034 m^{-1} to

$$\Delta a = \{[(0.71)(0.00486)]^2 + 0 + 0 + [(1) \times (0.005)]^2\}^{1/2}\ \text{m}^{-1} = 0.0061\ \text{m}^{-1}. \quad (16)$$

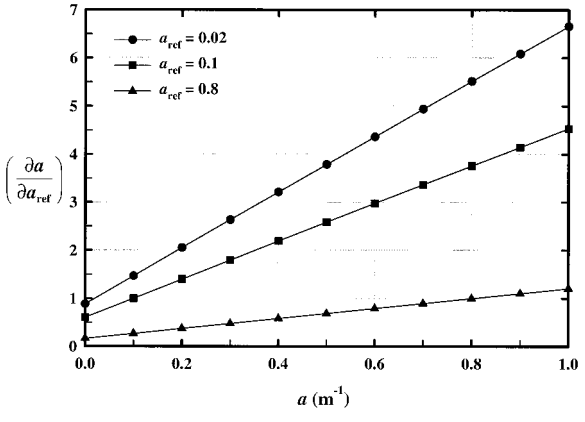

Fig. 7. Sensitivity coefficient $\partial a/\partial a_{\text{ref}}$ when ρ is known for $r = 0.05$ m and ρ = 0.99.

Table 2. Sensitivity Coefficients for the Determination of a with Eqs. (6)–(10) when ρ is Unknown[a]

Coefficient	Value
$\partial a/\partial T$	$-0.72\ \text{m}^{-1}$
$\partial a/\partial a_{\text{ref}}$ $(B \neq R)$	2.1
$\partial a/\partial T_{AB}$	$0.83\ \text{m}^{-1}$
$\partial a/\partial a_A$	4.2
$\partial a/\partial a_B$ $(B \neq R)$	−5.3
$\partial a/\partial r$	$-0.0026\ \text{m}^{-2}$
$\partial a/\partial a_{\text{ref}}$ $(B = R)$	−1.2
$(T)(\partial a/\partial T)$	$-0.35\ \text{m}^{-1}$
$(a_{\text{ref}}/a)(\partial a/\partial a_{\text{ref}})$	0.21
$(T_{AB})(\partial a/\partial T_{AB})$	$0.56\ \text{m}^{-1}$
$(a_A/a)(\partial a/\partial a_A)$	2.1
$(a_B/a)(\partial a/\partial a_B)$	−2.6
$(r/a)(\partial a/\partial r)$	-6.5×10^{-4}
$(a_{\text{ref}}/a)(\partial a/\partial a_{\text{ref}})$	−0.12

[a] $a = 0.2\ \text{m}^{-1}$, $a_{\text{ref}} = 0.02\ \text{m}^{-1}$, $r = 0.05$ m, ρ = 0.99, $a_A = 0.1\ \text{m}^{-1}$, and $a_B = 0.05\ \text{m}^{-1}$.

Admittedly, however, it may be prohibitively difficult to produce many reference solutions. Also note that, although $\partial a/\partial \rho$ is theoretically zero when $a = a_{\text{ref}}$, the slope of $\partial a/\partial \rho$ versus a (Fig. 5) is in some cases so steep that the uncertainty in a_{ref} introduces a significant uncertainty in $\partial a/\partial \rho$.

B. Unknown ρ

If the value of ρ to be used in Eq. (10) is unknown it can be determined with Eq. (9). In this case our estimate of a ultimately depends on the measurements of r, a_A, a_B, T_{AB}, a_{ref}, and T. The value of the sensitivity coefficient $\partial a/\partial T$ is the same as that given in Subsection 4.A [Eq. (11) and Fig. 4]. The value of $\partial a/\partial a_{\text{ref}}$, on the other hand, is the same as that given in Subsection 4.A only if the reference sample B used in the determination of ρ [Eq. (9)] is not chosen to be the same as the reference sample R used in the determination of a [Eq. (10)]. Because the measurement T_{AB} depends on r, the value of $\partial a/\partial r$ is not the same as that given in Subsection 4.A. We therefore need to determine the new sensitivity coefficients $\partial a/\partial r$, $\partial a/\partial a_A$, $\partial a/\partial a_B$, $\partial a/\partial T_{AB}$, and, when R and B are the same fluid, $\partial a/\partial a_{\text{ref}}$. Each new sensitivity coefficient depends in general on the six physical parameters r, ρ, a_A, a_B, a_{ref}, and a.

We know from Subsection 4.A that for the special case of $a_{\text{ref}} = a$ the values of ρ and r in Eq. (10) have no effect on the estimate of a. Because the values of a_A, a_B, and T_{AB} affect a only through ρ, these three measurements are unimportant, and therefore ineffective, when $a_{\text{ref}} = a$. Therefore we no longer want to set $a_{\text{ref}} \approx a$ when using Eqs. (9) and (10) in combination. Instead we take advantage of the fact that Eq. (9) is the inverse of Eq. (10). The measurement error in r tends to cancel when these equations are used in combination. Likewise, if we take R and B to be the same solution, then the estimate of a will be relatively insensitive to the measurement of a_{ref}.

Table 2 gives the values of the sensitivity coefficients, both in their unnormalized and in their nor-

malized form, for the case of $a = 0.2\ \mathrm{m}^{-1}$, $a_{\mathrm{ref}} = 0.02\ \mathrm{m}^{-1}$, $a_A = 0.1\ \mathrm{m}^{-1}$, $a_B = 0.05\ \mathrm{m}^{-1}$, $r = 0.05$ m, and $\rho = 0.99$. Note that all the sensitivity coefficients have relatively small values compared with that of $\partial a/\partial\rho$ from Eq. (10) alone (Table 1). Also note in Table 2 that $\partial a/\partial r$ is now $-0.0026\ \mathrm{m}^{-2}$, compared with $-3.2\ \mathrm{m}^{-2}$ in Table 1, verifying that the precision of the measurement of r is even less important when a is determined with Eqs. (9) and (10) together than when a is found from Eq. (10) alone. (The uncertainty of r is unlikely to be important in either case.) Furthermore, we can see from Table 2 that $\partial a/\partial a_{\mathrm{ref}}$ when $B = R$ is smaller than either $\partial a/\partial a_{\mathrm{ref}}$ or $\partial a/\partial a_B$ when $B \neq R$, confirming that we should let B and R be the same solution. Accordingly, we assume that $B = R$ for the remainder of this subsection. Ignoring Δr, we obtain the uncertainty in a from

$$\Delta a = \left[\left(T\frac{\partial a}{\partial T}\right)^2\left(\frac{\Delta T}{T}\right)^2 + \left(\frac{\partial a}{\partial a_{\mathrm{ref}}}\right)^2(\Delta a_{\mathrm{ref}})^2 + \left(T_{AB}\frac{\partial a}{\partial T_{AB}}\right)^2\left(\frac{\Delta T_{AB}}{T_{AB}}\right)^2 + \left(\frac{\partial a}{\partial a_A}\right)^2(\Delta a_A)^2\right]^{1/2}. \tag{17}$$

If, for the example used in Table 2, we measure a_{ref} ($0.02\ \mathrm{m}^{-1}$) and a_A ($0.1\ \mathrm{m}^{-1}$) each to $\pm 0.005\ \mathrm{m}^{-1}$ and the corresponding values of T and T_{AB} each to $\pm 1\%$, then from Eq. (17) and Table 2 we obtain

$$\begin{aligned}\Delta a &= \{[(0.35)(0.01)]^2 + [(1.2)(0.005)]^2 + [(0.56)\times(0.01)]^2 + [(4.2)(0.005)]^2\}^{1/2}\ \mathrm{m}^{-1}\\ &= (1.2\times 10^{-5} + 3.6\times 10^{-5} + 3.1\times 10^{-5} + 4.4\times 10^{-4})^{1/2}\ \mathrm{m}^{-1} = 0.023\ \mathrm{m}^{-1}.\end{aligned} \tag{18}$$

Here the uncertainty in a is due mostly to the uncertainty in a_A. The calculated value of a ($0.200 \pm 0.036\ \mathrm{m}^{-1}$) is an improvement over the example given in Eq. (15), indicating that even if the value of ρ is known from direct measurement it may be prudent to use Eq. (9) to determine the value of ρ for use in Eq. (10) rather than the measured value of ρ. Because the experimental setup is the same for Eqs. (9) and (10), the uncertainties in the physical parameters are far less important when a combination of Eqs. (9) and (10) is used than when Eq. (10) is used alone. Even if the directly measured value of ρ is more accurate than the value of ρ obtained from Eq. (9), it generally will not lead to a more accurate value of a when used in Eq. (10).

The derivation of general expressions for the sensitivity coefficients for Eqs. (9) and (10) is outlined in Appendix B. The value of $\partial a/\partial r$ was found to be negligibly small over a wide range of physical parameters and is identically zero when $a = a_A$. Although an error in r results in an error in ρ with Eq. (9), the errors in r and ρ are such that their effects cancel each other in the determination of a with Eq. (10). The value of $\partial a/\partial a_{\mathrm{ref}}$ is also zero when $a_A = a$. Therefore the estimate of a from Eqs. (9) and (10) depends only on the measurements of T, T_{AB}, and a_A when $a_A \approx a$.

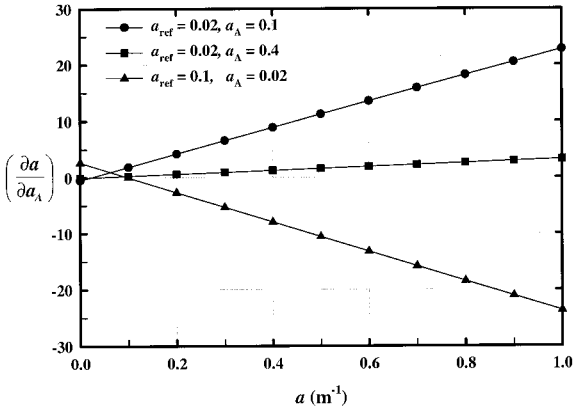

Fig. 8. Sensitivity coefficient $\partial a/\partial a_A$ for $r = 0.05$ m and $\rho = 0.99$.

As illustrated in Fig. 8 the value of $\partial a/\partial a_A$ is approximately linearly dependent on a and equals zero when $a = a_{\mathrm{ref}}$. The slope of the $\partial a/\partial a_A$ curve versus the a curve is larger for small values of a_A (i.e., $a_A > a$) than for large values of a_A. It is positive when $a_A > a_{\mathrm{ref}}$ and negative when $a_A < a_{\mathrm{ref}}$. Similarly, as shown in Fig. 9, the value of $T_{AB}(\partial a/\partial T_{AB})$ is approximately linearly dependent on a and equals zero when $a = a_{\mathrm{ref}}$. The slope of $(T_{AB}\partial a/\partial T_{AB})$ versus a is positive when $a_A > a_{\mathrm{ref}}$ and negative when $a_A < a_{\mathrm{ref}}$.

We conclude that it is desirable for a_A to be at least as large as a. For $a_A > a$, we are faced with a trade-off: increasing a_A generally decreases the sensitivity of a to both a_A and T_{AB} but increases its sensitivity to a_{ref}.

5. Nondiffuse Source

Up to this point in our analysis we have assumed that the PSICAM is illuminated with a perfectly isotropic source. However, a small isotropic source is technically difficult to construct. Therefore in this section we evaluate the performance of a PSICAM when the source is anisotropic. Three-dimensional Monte

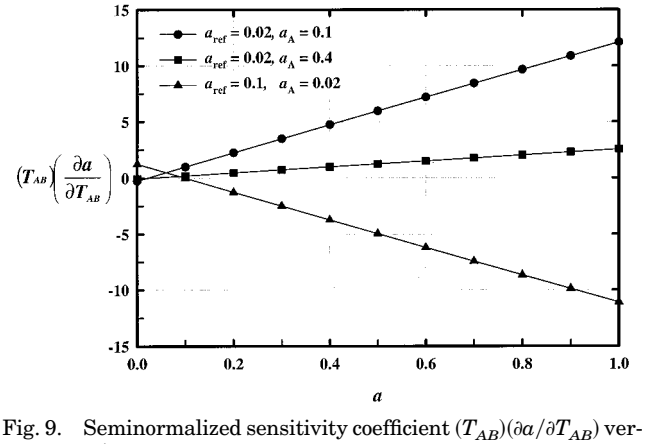

Fig. 9. Seminormalized sensitivity coefficient $(T_{AB})(\partial a/\partial T_{AB})$ versus a (m^{-1}) for $r = 0.05$ m and $\rho = 0.99$.

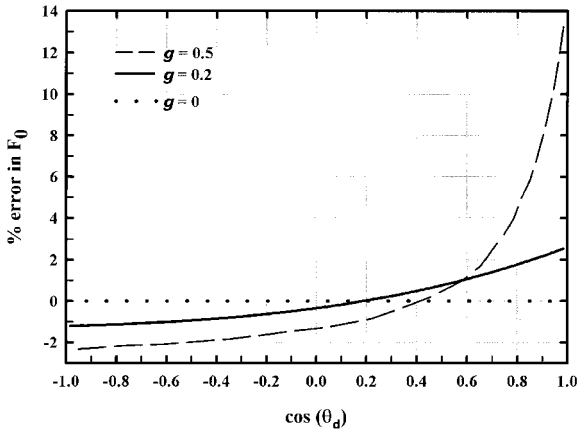

Fig. 10. Percentage error in the PSICAM detector response as a function of detector location for anisotropic light sources. The detector position is given by angle θ_d with respect to the forward direction of the source. The source angular distribution is the Henyey–Greenstein function with asymmetry factors $g = 0$, 0.2, and 0.5. The results shown are for $a = 0.3\ \mathrm{m}^{-1}$, $b = 0.7\ \mathrm{m}^{-1}$, $r = 0.05$ m, and $\rho = 0.99$.

Carlo simulations were performed for several different types of centrally located source, and the wall irradiance was determined at various sections of the PSICAM wall. It is important to note that the total irradiance incident on the entire cavity wall is independent of the shape of the source function; however, the irradiance at a particular location on the wall, and therefore at the detector, does depend on the source shape.

Shown in Fig. 10 is the percentage error in PSICAM detector irradiance for central light sources that are characterized by the Henyey–Greenstein function [analogous to Eq. (A4)] for asymmetry factor values of $g = 0$, 0.2, and 0.5 and for $r = 0.05$ m, $\rho = 0.99$, $a = 0.3\ \mathrm{m}^{-1}$, and $b = 0.7\ \mathrm{m}^{-1}$. The error is plotted against the position of the detector, expressed in terms of the angle θ_d between the forward direction of the light source and the radius from the center to the detector. (For example, $\theta_d = 0$ when the source is pointed straight at the detector.) If the source is perfectly isotropic, the irradiance is identical at all positions on the cavity wall and the error that is due to the source is zero everywhere. For a source characterized by the Henyey–Greenstein function, the irradiance is stronger than that for an isotropic source at small values of θ_d, whereas the irradiance is weaker than that for an isotropic source at large values of θ_d. For a source with $g = 0.2$, 65% of the total source light is projected in the forward 180 deg, most of which is concentrated in the near-forward directions, and 35% is projected in the backward 180 deg. However, because of the large number of wall reflections, in this case 33, the error in the wall irradiance is less than 2.5% at all locations. It can be seen from Fig. 10 that it would be best to place the detector at approximately a right angle to the sensor, where the error that is due to the source is near zero. For a source with $g = 0.5$, 83% of the source light is projected in the forward 180 deg and 17% in the backward directions. Although this extremely anisotropic source would not be practical, we conclude from Fig. 10 that, theoretically, it could be used if the detector were placed near $\theta_d = 60°$.

It is important to note that the error in T or T_{AB} may be much smaller than the error in the detector response. If the detector receives more source light than it would with a perfectly isotropic source, it will do so both with the reference fluid and with the sample of interest. The error will not completely cancel out, however, because the amount of scattering and the average number of wall reflections will be different in the reference than in the sample.

In summary we conclude that, although it is not critical to construct the light source to be perfectly isotropic, the error that is due to this anisotropy should be minimized when the irradiance sensor is positioned at a location where the source strength is near its average value.

If a sufficiently isotropic source cannot be obtained, it may be preferable to replace the plane irradiance sensor with a radiance sensor that is positioned such that the source is not within the detector's field of view. In this case Eq. (2) would be replaced with

$$N_C = \frac{\rho P_0 P_s}{1 - \rho P_s}, \tag{19}$$

an approximation that ignores the scattering of light during its first pass from the source to the wall. We will quantify the accuracy of Eq. (19) in a future paper.

6. Conclusions

Consistent with Kirk,[9,10] we found that the scattering errors in Eqs. (4) and (6) are insignificant for most ocean optics problems. However, as demonstrated in Figs. 1–3, the scattering errors may be important for near-IR light or for other PSICAM applications.

If the value of the PSICAM wall reflectivity is known, the absorption coefficient of a sample can be determined [with Eq. (10)] from PSICAM measurements of the sample and of a reference solution. Because of the high sensitivity of a to ρ, however, the uncertainty in the result may be unacceptably large unless ρ is known to high precision and $a \approx a_{\mathrm{ref}}$. On the other hand, we can obtain a precise determination of a by producing a nonscattering dye solution such that $T = 1$ and by determining the value of a_{ref} with a spectrophotometer.

Alternatively, we can obtain a generally more precise result by including the PSICAM measurement of at least one additional reference solution, eliminating the need to know the value of the wall reflectivity *a priori*. Even if the value of ρ is known from direct measurement, it may be preferable to determine it with Eq. (9) because this tends to eliminate errors associated with the measurements of ρ, r, and a_{ref}.

A prototype PSICAM is currently under construction, and we intend to publish a description of the instrument design and laboratory experiments once they have been completed. We will also present an

analysis of a PSICAM in which a radiance sensor is used [with Eq. (19)] in place of a plane irradiance sensor. A radiance sensor is easier to implement and may reduce errors associated with a nonisotropic light source; however, it also introduces a new source of scattering error. The significance of the scattering error must be evaluated for the range of ocean water types before one can safely adopt the radiance approach.

Appendix A: Monte Carlo Techniques

In the Monte Carlo simulations photons were traced one at a time and the light field was taken to be the superposition of all the photon paths. The path of each photon was determined by random numbers $\mathcal{R}$ evenly distributed in the range [0, 1]. The photon path length s was found from

$$s = -(1/c)\ln(1 - \mathcal{R}), \tag{A1}$$

where c is the attenuation coefficient (1/m). At each scattering event, the azimuthal scattering angle with respect to the incident direction was found with

$$\Phi = 2\pi\mathcal{R}. \tag{A2}$$

For isotropic scattering, the cosine of the polar scattering angle with respect to the incident direction μ_s was found with

$$\mu_s = 1 - 2\mathcal{R}. \tag{A3}$$

For Henyey–Greenstein scattering[13,14]

$$\tilde{\beta}(g; \mu_s) \equiv \frac{1}{4\pi}\frac{1 - g^2}{(1 + g^2 - 2g\mu_s)^{3/2}}, \tag{A4}$$

where g is the scattering asymmetry factor. The corresponding cumulative distribution function is

$$C(\mu_s) = \frac{1}{2}\int_{\mu_s}^{1}\frac{1 - g^2}{(1 + g^2 - 2g\mu_s)^{3/2}} = \frac{1 - g^2}{2g}\left[\frac{1}{1 - g} - \frac{1}{(1 + g^2 - 2g\mu_s)^{1/2}}\right]. \tag{A5}$$

Setting $\mathcal{R}$ equal to the cumulative distribution function and solving for μ_s, we found μ_s with

$$\mu_s = \frac{2g + 1 - 2\mathcal{R}g - 2\mathcal{R} + 2\mathcal{R}^2g + g^2 - 2g^3\mathcal{R} - 2\mathcal{R}g^2 + 2g^3\mathcal{R}^2}{(-g - 1 + 2\mathcal{R}g)^2}. \tag{A6}$$

For Petzold scattering, we solved for μ_s with

$$C(\mu_s) = \mathcal{R}, \tag{A7}$$

where the cumulative distribution function $C(\mu_s)$ was taken to be the average of those provided by Petzold[11] for the three samples from San Diego Harbor.

For each scattering event, the new direction cosines of the photon $(\alpha', \beta', \gamma')$ were computed from the initial photon direction cosines (α, β, γ) and scattering angles (polar angle Θ, azimuthal angle Φ) with

$$\begin{bmatrix}\alpha'\\ \beta'\\ \gamma'\end{bmatrix} = \begin{bmatrix}\alpha\gamma/\sqrt{1-\gamma^2} & -\beta/\sqrt{1-\gamma^2} & \alpha\\ \beta\gamma/\sqrt{1-\gamma^2} & \alpha/\sqrt{1-\gamma^2} & \beta\\ -\sqrt{1-\gamma^2} & 0 & \gamma\end{bmatrix} \times \begin{bmatrix}\alpha_s\\ \beta_s\\ \gamma_s\end{bmatrix}, \quad (\gamma^2 < 1), \tag{A8}$$

$$\begin{bmatrix}\alpha'\\ \beta'\\ \gamma'\end{bmatrix} = \mathrm{sign}(\gamma)\begin{bmatrix}\alpha_s\\ \beta_s\\ \gamma_s\end{bmatrix}, \quad (\gamma^2 = 1), \tag{A9}$$

where

$$\alpha_s = \sin(\Theta)\cos(\Phi), \quad \beta_s = \sin(\Theta)\sin(\Phi), \quad \gamma_s = \cos(\Theta). \tag{A10}$$

Appendix B: Sensitivity Coefficients when ρ is Known

Let T_4 designate $T(a, a_{\mathrm{ref}}, r, \rho)$ as given by Eq. (10):

$$T_4 \equiv T(a, a_{\mathrm{ref}}, r, \rho). \tag{B1}$$

The derivatives $\partial a/\partial T$ and $\partial a/\partial a_{\mathrm{ref}}$ $(B \neq R)$ are the same as those given in Subsection 4.A:

$$\frac{\partial a}{\partial T_4}(a, a_{\mathrm{ref}}, r, \rho) = 1\Big/\left(\frac{\partial T_4}{\partial a}\right), \tag{B2}$$

$$\frac{\partial a}{\partial a_{\mathrm{ref}}}(a, a_{\mathrm{ref}}, r, \rho) = -\left(\frac{\partial T_4}{\partial a_{\mathrm{ref}}}\right)\Big/\left(\frac{\partial T_4}{\partial a}\right), (B \neq R). \tag{B3}$$

The other sensitivity coefficients, however, depend on six parameters: interchangeably $(a, a_{\mathrm{ref}}, r, a_A, a_B, T_{AB})$ or $(a, a_{\mathrm{ref}}, r, a_A, a_B, \rho)$. Let $\rho(a_A, a_B, r, T_{AB})$ be given by Eq. (9) and $T_{AB}(a_A, a_B, r, \rho)$ be given by Eq. (3). We can substitute $\rho(a_A, a_B, r, T_{AB})$ into the expression for $T(a, a_{\mathrm{ref}}, r, \rho)$ and thereby express T in terms of six parameters:

$$T_6 \equiv T(a, a_{\mathrm{ref}}, r, a_A, a_B, T_{AB}). \tag{B4}$$

Each of the sensitivity coefficients can be determined either directly from T_6 or from a combination of T_4 and ρ as follows:

$$\frac{\partial T}{\partial r}(a, a_{\mathrm{ref}}, r, a_A, a_B, \rho) = \frac{\partial T_6}{\partial r} = \frac{\partial T_4}{\partial r} + \frac{\partial T_4}{\partial \rho}\frac{\partial \rho}{\partial r}, \tag{B5}$$

$$\frac{\partial a}{\partial r}(a, a_{\mathrm{ref}}, r, a_A, a_B, \rho) = -(\partial T_6/\partial r)/(\partial T_6/\partial a) = -\left(\frac{\partial T_4}{\partial r} + \frac{\partial T_4}{\partial \rho}\frac{\partial \rho}{\partial r}\right)\Big/(\partial T_4/(\partial a), \quad \text{(B6)}$$

$$\frac{\partial a}{\partial a_A}(a, a_{\mathrm{ref}}, r, a_A, a_B, \rho) = -(\partial T_6/\partial a_A)/(\partial T_4/\partial a) = -[(\partial T_4/\partial \rho)(\partial \rho/\partial a_A)]/(\partial T_4/\partial a), \quad \text{(B7)}$$

$$\frac{\partial a}{\partial a_B}(a, a_{\mathrm{ref}}, r, a_A, a_B, \rho) = -(\partial T_6/\partial a_B)/(\partial T_4/\partial a) = -[(\partial T_4/\partial \rho)(\partial \rho/\partial a_B)]/(\partial T_4/\partial a), \quad \text{(B8)}$$

$$\frac{\partial a}{\partial T_{AB}}(a, a_{\mathrm{ref}}, r, a_A, a_B, \rho) = -(\partial T_6/\partial T_{AB})/(\partial T_4/\partial a) = -[(\partial T_4/\partial \rho)(\partial \rho/\partial T_{AB})]/(\partial T_4/\partial a), \quad \text{(B9)}$$

If the same reference solution is used in Eqs. (9) and (10) (i.e., $B = R$), then T can be expressed in terms of five parameters:

$$T_5 = T(a, a_{\mathrm{ref}}, r, a_A, T_{AB}), \quad \text{(B10)}$$

and the sensitivity coefficient for a_{ref} becomes

$$\frac{\partial a}{\partial a_{\mathrm{ref}}}(a, a_{\mathrm{ref}}, r, a_A, \rho) = -\left(\frac{\partial T_5}{\partial a_{\mathrm{ref}}}\right)\Big/\left(\frac{\partial T_4}{\partial a}\right) = \left[\frac{\partial T_4}{\partial a_{\mathrm{ref}}} + \left(\frac{\partial T_4}{\partial \rho}\right)\left(\frac{\partial \rho}{\partial a_{\mathrm{ref}}}\right)\right]\Big/\left(\frac{\partial T_4}{\partial a}\right). \quad \text{(B11)}$$

This research was inspired by a presentation by John Kirk at the European Joint Research Center in Ispra, Italy, in July 1999. We gratefully acknowledge the support of the U.S. Office of Naval Research and thank the reviewers and Alan Weidemann for their helpful suggestions.

References

1. C. S. Roesler, "Theoretical and experimental approaches to improve the accuracy of particulate absorption coefficients derived from the quantitative filter technique," Limnol. Oceanogr. **43,** 1649–1660 (1998).
2. C. Moore, "In situ biochemical, oceanic, optical meters," Sea Technol. **35,** 10–16 (1994).
3. M. S. Twardowski, J. M. Sullivan, P. L. Donaghay, and J. R. V. Zaneveld, "Microscale quantification of the absorption by dissolved and particulate material in coastal waters with an ac-9," J. Atmos. Oceanic Technol. **16,** 691–707 (1999).
4. H. R. Gordon and G. C. Boynton, "Radiance–irradiance inversion algorithm for estimating the absorption and backscattering coefficients of natural waters: vertically stratified water bodies," Appl. Opt. **37,** 3886–3896 (1998).
5. R. A. Leathers, C. S. Roesler, and N. J. McCormick, "Ocean inherent optical property determination from in-water light measurements," Appl. Opt. **38,** 5096–5103 (1999).
6. P. Elterman, "Integrating cavity spectroscopy," Appl. Opt. **9,** 2140–2142 (1970).
7. E. S. Fry and G. Kattawar, "Measurement of the absorption coefficient of ocean water using isotropic illumination," in *Ocean Optics IX*, M. A. Blizard, ed., Proc. SPIE **925,** 142–148 (1988).
8. E. S. Fry, G. Kattawar, and R. M. Pope, "Integrating cavity absorption meter," Appl. Opt. **31,** 2055–2065 (1992).
9. J. T. O. Kirk, "Modeling the performance of an integrating-cavity absorption meter: theory and calculations for a spherical cavity," Appl. Opt. **34,** 4397–4408 (1995).
10. J. T. O. Kirk, "Point-source integrating-cavity absorption meter: theoretical principles and numerical modeling," Appl. Opt. **36,** 6123–6128 (1997).
11. T. J. Petzold, "Volume scattering functions for selected ocean waters," SIO Ref. 72–78 (Scripps Institution of Oceanography, La Jolla, Calif., 1972).
12. P. R. Bevington and D. K. Robinson, *Data Reduction and Error Analysis for the Physical Sciences* (McGraw-Hill, New York, 1992).
13. L. C. Henyey and J. L. Greenstein, "Diffuse radiation in the galaxy," Astrophys. J. **93,** 70–83 (1941).
14. C. D. Mobley, *Light and Water. Radiative Transfer in Natural Waters* (Academic, New York, 1994).